Tribology and Materials
Vol. 4, No. 3, 2025, pp. 144-154

ISSN 2812-9717
https://doi.org/10.46793/tribomat.2025.015

Microstructure, hardness and tribological behaviour of plasma nitrided R260 rail steel with different nitrogen and hydrogen gas mixtures

Ahmet DEVECI, Harun MINDIVAN*

Bilecik Şeyh Edebali University, Bilecik, Turkey
*Corresponding author: harun.mindivan@bilecik.edu.tr

Keywords
pearlitic rail steel
plasma nitriding
compound layer
gas mixture influence
wear

History
Received: 08-10-2024
Revised: 09-12-2024
Accepted: 05-01-2025

Abstract

Railway components are essential parts of transportation infrastructure, withstanding complex and dynamic loads during their operational lifespan. This work aims to improve the wear resistance of railway rails by investigating the correlation between the microstructure, hardness and tribological behaviour of R260 pearlitic rail steel. This will be achieved through a twelve-hour plasma nitriding process at a temperature of 450 °C, using two different N_2-H_2 gas mixtures (20 vol. % N_2 + 80 vol. % H_2 and 80 vol. % N_2 + 20 vol. % H_2). The treated surfaces were characterised using light optical microscopy, scanning electron microscopy, X-ray diffraction and microhardness testing. The unlubricated tribological behaviour of plasma-nitrided steel was investigated in a ball-on-flat tribometer at room temperature. The 20 and 80 vol. % N_2 gas mixture led to a biphasic compound layer of ε-$Fe_{2-3}N$ and γ'-Fe_4N. As the amount of nitrogen in the gas mixture increased, the total compound layer, surface roughness and surface residual compressive stress increased. In the tribological tests, the steel treated with a nitrogen-rich gas mixture (80 vol. % N_2) yielded better results due to the formation of a thicker compound layer, a deeper case-hardening and higher compressive residual stress within the nitride layer.

1. Introduction

With countries' economies growing, the average speed of trains and load-carrying requirements have significantly increased. A great deal of attention has been drawn to the fact that the severity of the damage to the rails has increased together with the increase in the axle load and speed of the train. In practice, various types of rail damages, such as rail side wear, rail corrugation, fatigue cracks and spalling, add to the track maintenance and replacement cost [1]. Additionally, these maintenance operations disrupt the train's running schedule. Pearlitic rails' inferior toughness also causes cracks and damage during handling, transport and storage. These severe service conditions require rails with higher strength and toughness, as well as improved wear and fatigue resistance [2]. The relationship between hardness and resistance to wear and rolling contact fatigue (RCF) is evident. Higher hardness steels show improved RCF resistance. Bainitic steels show reduced wear resistance but higher RCF resistance [3].

Surface treatments, including rail grinding, laser cladding, hardening and the application of coatings, are recognised for enhancing the wear and RCF characteristics of rail materials. Gas nitriding of the wheel and rail rollers increases surface hardness to above 800 HV. Consequently, they exhibit greater resistance to RCF and wear at the wheel-rail contacts [4]. Nitriding forms a hard exterior compound layer on the surface, accompanied by an underlying diffusion zone. The compound layer consists of γ'-Fe_4N and/or ε-$Fe_{2-3}N$-type iron nitrides, while the

diffusion zone comprises a nitrogen-rich solid solution zone including fine and coherent nitride precipitates [5]. The compound layer imparts tribological properties and corrosion resistance, whereas the diffusion zone determines the fatigue strength of the nitrided layer. Research indicates that the ε-nitride in the compound layer exhibits superior wear resistance compared to the γ'-nitride due to its compact structure of densely packed hexagonal arrangements and elevated nitrogen concentration [6]. Landgraf et al. [7] investigated the nitrided zones of high-alloy tool steel X153CrMoV12 at varying temperatures and treatment times. The study reveals that the distribution of carbides affects the diffusion of nitrogen and layer growth, with higher temperatures leading to increased layer thickness. A new finite element analysis methodology was developed to map the heterogeneous nitrogen evolution and distribution.

Dalcin et al. [8] studied the sliding wear of DIN 18MnCrSiMo6-4 continuous cooling bainitic steel plasma nitrided with nitrogen-rich gas composition. They found that plasma nitrided samples at 550 °C showed better wear performance due to a thicker compound layer and higher diffusion zone. Another study by Dalcin et al. [9] also examined the impact of gas mixture on the first damage resistance of plasma nitrided DIN 18MnCrSiMo6-4 bainitic steel, finding that increasing nitrogen content led to brittle behaviour. Dalcin et al. [10] also studied forged gears using bainitic steel and plasma nitriding treatments. They found that nitrogen-rich gas composition increased surface hardness but decreased fracture toughness, with 24 vol. % N_2 achieving the best performance. Contrary to the established beneficial impact of nitriding in protecting surfaces from mechanical wear, certain research [11] has indicated that the brittle ε-nitride in the compound layer accelerates the wear of nitrided steels during sliding. With regard to the RCF or wear performance of the nitriding treatment on wheel-rail surfaces, there has been no report as of yet.

The present investigation aimed to develop plasma nitriding on selected rail steel (R260). The plasma nitriding was developed in a gas mixture of N_2:H_2 at 20:80 and 80:20 (vol. % ratio) at a fixed time and temperature. After plasma nitriding, the in-depth characterisation of the untreated and surface-treated steels was carried out. Subsequently, tribological tests were carried out on a reciprocating ball-on-flat method following the ASTM G133 standard. The current research work aimed to observe the effect of higher loads (45 and 60 N) on the dry sliding tribological behaviour of plasma-nitrided rail steel.

2. Material and methods

Experimental work was carried out on an R260 rail steel, which underwent machining on a lathe without any further heat treatment. The mechanically hardened layer was removed using 220 to 2000 grit emery sheets. Grinding reduced average surface roughness (*Ra*) to 0.12 µm before surface treatments. Table 1 shows steel's chemical composition. The rail steel has pearlite (lamellae of cementite and ferrite) microstructure with a hardness of 330 HV0.01, as shown in Figure 1. The rail steel is eutectoid steel because the carbon content of rail is approximately 0.7 wt. % (Table 1). All samples were cleaned with acetone in an ultrasonic cleaner and air-dried before plasma nitriding to remove oxide from the surface.

Table 1. Chemical composition of rail steel

Element	C	Mn	Cr	Mo	Fe
wt. %	0.6 – 0.8	0.13 – 0.6	0.15	0.02	balance

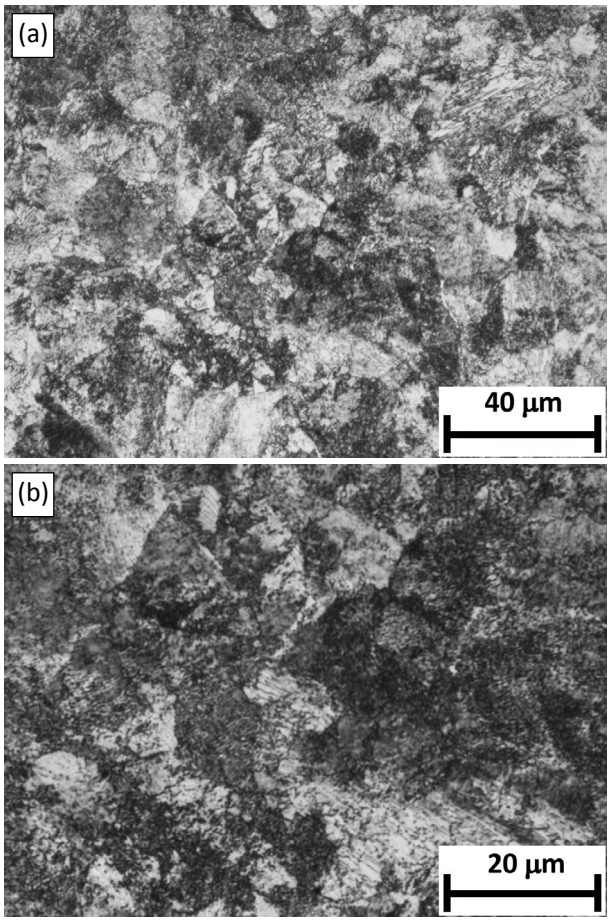

Figure 1. LOM images of the microstructure of as-received rail material at: (a) lower magnification and (b) higher magnification

The plasma nitriding technique was used under two distinct circumstances, with conditions shown in Table 2. The samples were vacuumed until the process chamber pressure reached 2 Pa before the nitriding procedure was performed on the cathode. In order to prepare the surface for nitriding, it was necessary to introduce hydrogen gas into the interior until the gas pressure reached 250 Pa. This procedure, known as the "scattering process", cleaned and roughened the surface. A treatment temperature of 250 °C was used for 30 minutes of scattering. After this process, samples were nitrided at a temperature of 450 °C for 12 hours, using a gas mixture consisting of 20 vol. % N_2 + 80 vol. % H_2 and 80 vol. % N_2 + 20 vol. % H_2. The samples were then slowly placed into a vacuum chamber and cooled down to room temperature. The nitrided samples were then cut into sections, mounted in bakelite, ground, polished (1 µm Al_2O_3) and etched with 2 % Nital (2 vol. % HNO_3 + 98 vol. % CH_3CH_2OH).

Table 2. Plasma nitriding test parameters

Sample	Temperature, °C	Time, hours	N_2:H_2
PN1	450	12	20:80
PN2			80:20

The structural analyses of the cross-sections of the nitrided surfaces were examined by a Nikon Eclipse LV150 light optical microscope (LOM) and a Zeiss Supra 40VP scanning electron microscope (SEM) equipped with energy-dispersive X-ray spectrometer (EDX). Phase analyses of the treated surfaces were made with a Panalytical Empyrean X-ray diffractometer (XRD) using CuKα radiation in the 2θ° range of 30 – 95° at a step of 0.020° and a scanning speed of 1°/min. The physical properties of the diffusion layer as a function of depth were characterised, and the thickness of the diffusion layer was determined using microhardness measurements. The hardness measurements were done on the cross-sections of the treated surfaces using a Vickers microhardness tester (Shimadzu HVM) with a load of 10 g, according to the ASTM E92 standard [12]. The average arithmetic mean deviation (*Ra*) and root mean square deviation (*Rq*) were measured using a contact profilometer (Mitutoyo Surftest SJ-400) in accordance with ISO 4287 standards [13].

Tribological tests (two repetitions for each condition) were carried out in the ambient condition (temperature 20 – 25 °C, humidity 40 – 50 %) using a custom-made tribometer with a reciprocating ball-on-flat configuration, according to the standard ASTM G133 [14]. In this configuration, an Al_2O_3 ball with a diameter of 10 mm slid forward and backwards against the sample with a sliding speed of 1.9 cm/s at loads of 15, 30, 45 and 60 N. The test's sliding amplitude (wear track length) of the reciprocating motion and overall sliding distance were 11.5 mm and 57.5 m, respectively. The tester's sensing cell automatically recorded the coefficient of friction (CoF). A surface profilometer (Mitutoyo Surftest SJ-400) measured the width and depth of the wear tracks to calculate the wear volume of the samples. The wear tracks were analysed by LOM.

3. Results and discussion

Figures 2 and 3 depict the LOM and SEM cross-sectional views of the steel treated at a temperature of 450 °C with gas mixtures (N_2:H_2) of 20:80 and 80:20, respectively. The research uncovered a microstructure in the surface layer of all plasma nitrided samples, consisting of a compound layer and a diffusion zone that extends

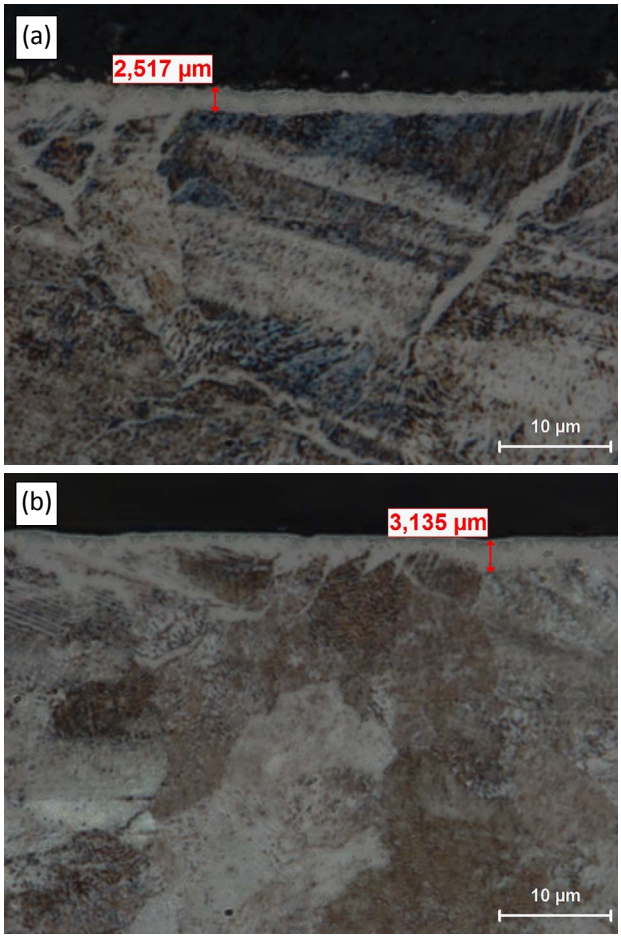

Figure 2. LOM images of the steel treated at a temperature of 450 °C with: (a) 20 vol. % N_2 and (b) 80 vol. % N_2

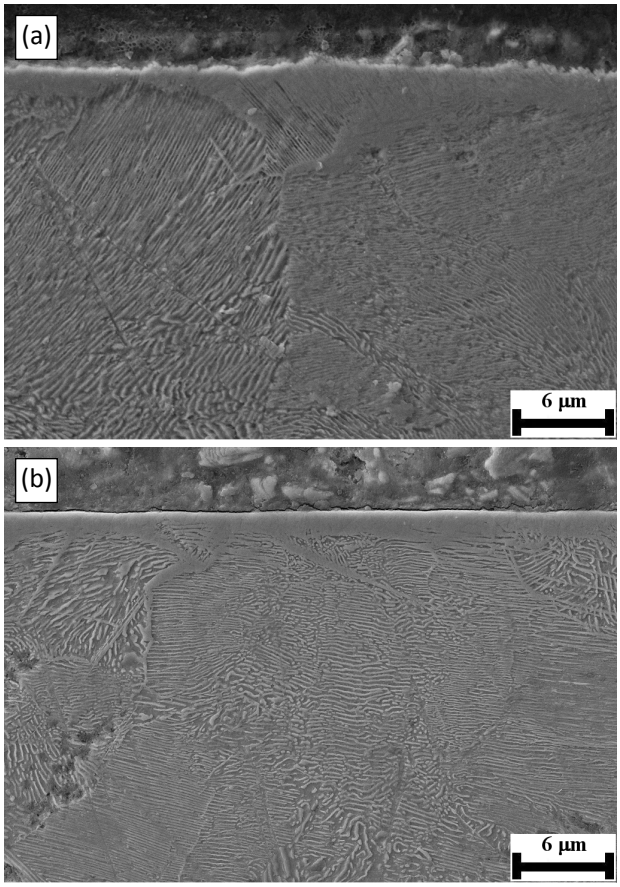

Figure 3. SEM images of the steel treated at a temperature of 450 °C with: (a) 20 vol. % N_2 and (b) 80 vol. % N_2

from the surface to the interior. The LOM and SEM images do not reveal the diffusion zone. As the N_2:H_2 gas ratio rises, the thickness of the compound layer increases (Fig. 4). This is because a higher amount of N_2 gas in the N_2-H_2 gas mixture causes more nitrogen atoms to diffuse into the surface. The types of chemical reactions occurring at the surface and the level of nitrogen diffusion influence the thickness and chemical composition of this surface layer during the plasma nitriding process [15]. Lower temperatures, such as 450 °C, limit the atomic nitrogen diffusion coefficient of a 20:80 gas mixture (N_2:H_2), in high-carbon steels like R260. This makes the compound layer and diffusion zone thinner. The steel treated with 20 vol. % N_2 has an average compound layer thickness of 2.58 ± 0.2 µm, as shown in Figure 4. However, for steel treated with 80 vol. % N_2, this value noticeably increases by approximately 110 %. The rise in N_2 gas amount in steel treated with 80 vol. % N_2 and its greater stability at lower temperatures clearly account for this increase.

Figure 5 shows the XRD patterns from the surface layer of the steel treated at a temperature of 450 °C with 20 and 80 vol. % N_2. The steel

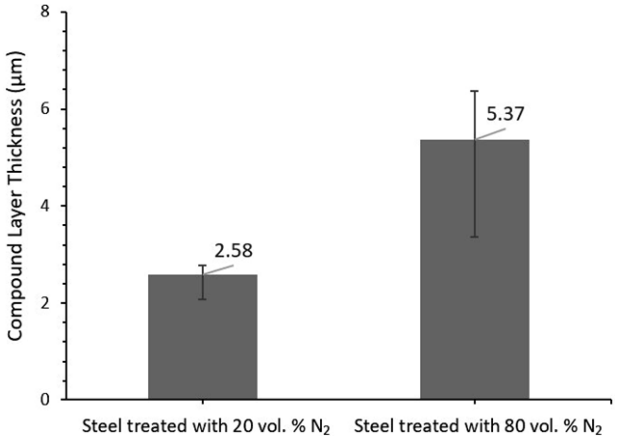

Figure 4. Compound layer thickness of steel treated at a temperature of 450 °C with 20 and 80 vol. % N_2

treated with 20 vol. % N_2 has a slightly enhanced diffraction peak intensity of the γ'-Fe_4N compared to that treated with 80 vol. % N_2. On the steel treated with 20 and 80 vol. % N_2, Figure 5 also shows the formation of a biphasic compound layer (ε-$Fe_{2-3}N$ and γ'-Fe_4N). It is deduced from Figures 4 and 5 that by increasing the N_2:H_2 gas mixture ratio and keeping the constant time of 12 hours, the α-Fe peak is eliminated from the XRD pattern due to an increase in the compound layer thickness. The incident X-ray cannot detect the α-Fe because the compound layer thickness is likely higher than the X-ray penetration depth [6]. These results show that altering the gas composition in N_2-H_2 plasma can control the phase structure and thickness in the compound layer. It should be noted that the peaks of α-Fe and nitrides are relatively weak for the gas composition of 20 vol. % N_2, probably due to the limited tendency of the diffused nitrogen to form the nitride phase at a lower amount of 20 vol. % N_2.

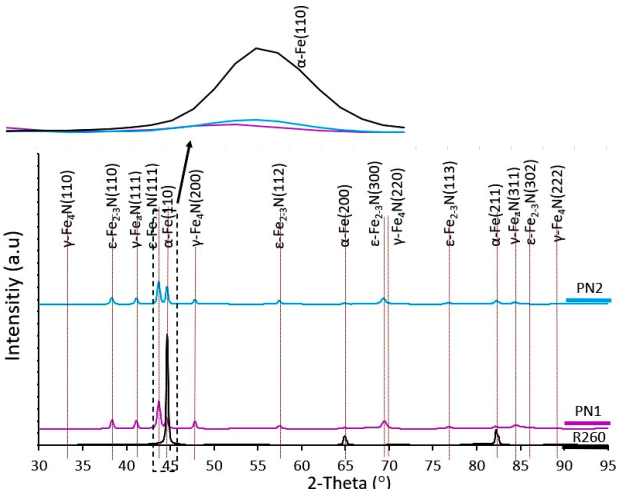

Figure 5. XRD patterns of the untreated R260 and steel treated at a temperature of 450 °C with 20 and 80 vol. % N_2

Additionally, compared to steel with a gas composition of 20 vol. % N_2, the α-Fe peaks of the steel with an 80 vol. % N_2 gas composition were broader and appeared at lower angles, indicating a higher dissolution of nitrogen atoms in the pearlitic matrix. Using Bragg's law ($n\lambda = 2d\sin\theta$), where d is the distance between planes, θ is the diffraction angle, n is a positive integer and λ is the XRD beam's wavelength, we can figure out the lattice parameters (a) of the untreated R260 and nitrided steel by using the main α-Fe peak (i.e. one that falls in the (110) diffraction plane) as a guide. Calculated average values for the untreated R260 and steel treated at 450 °C with 20 and 80 vol. % N_2 were 0.28723, 0.28776 and 0.29338 nm, respectively. Thus, dissolution of nitrogen atoms in α-Fe during the nitriding process caused a relative extension in the lattice parameter ($\Delta a/a$) of the matrix of about 0.18 % for the gas composition of 20 vol. % N_2 and 2.14 % for the gas composition of 80 vol. % N_2, as compared to the untreated R260 steel. This finding indicated the development of a larger compressive residual stress on the nitrogen-exposed surface of the steel treated at 450 °C with 80 vol. % N_2.

EDX point analysis is performed at different points in the compound layer and diffusion zone. The elemental point analysis at the surface level for the steel nitrided at a temperature of 450 °C with gas mixtures (N_2:H_2) of 20:80 and 80:20 are presented as X, Y and Z in Figure 6. The EDX analysis results marked as X and Y in the compound layer showed that this layer's outside and inside parts had different amounts of nitrogen. This confirmed the presence of two different types of iron nitride, i.e. ε-$Fe_{2-3}N$ and γ'-Fe_4N. In the diffusion zone, randomly oriented elongated light grey precipitates were observed, which are a common feature of nitrided steels (Fig. 2). According to the EDX analysis results marked as Z (Fig. 6b), elongated fine platelets identified as γ'-Fe_4N type iron nitrides (Fig. 2b), rather than randomly oriented long light grey platelets (Fig. 2a), predominate. Fig. 7 shows the typical elemental distribution along the layer depth of steel treated with 20 and 80 vol. % N_2.

Cross-section hardness measurements showed that the steel treated at a temperature of 450 °C with 20 and 80 vol. % N_2 had less hardness toward the substrate (Fig. 8). It has been demonstrated that the thickness of the nitride layer can be calculated as the thickness where the hardness value reaches the substrate hardness increased by 50 HV [16]. Hence, considering this fact, the thickness of the nitriding layer was found to be approximately 25 and 41 mm for steel treated at a temperature of 450 °C with 20 and 80 vol. % N_2, respectively.

Figure 9 shows the roughness values (parameters *Ra* and *Rq*) measured before and after plasma nitriding to investigate the influence of nitrogen gas composition on the surface topography. A gas composition containing 80 vol. % N_2 makes the surface of

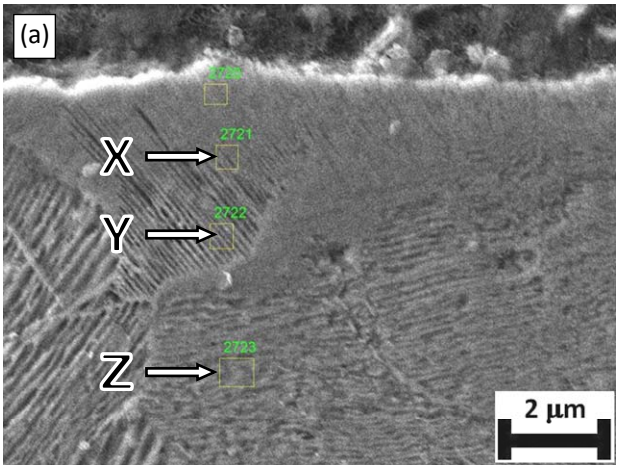

Element	Fe	C	N	Mn
X, at. %	82.70	9.99	6.52	0.79
Y, at. %	72.02	24.86	3.00	0.10
Z, at. %	81.49	17.59	0.05	0.87

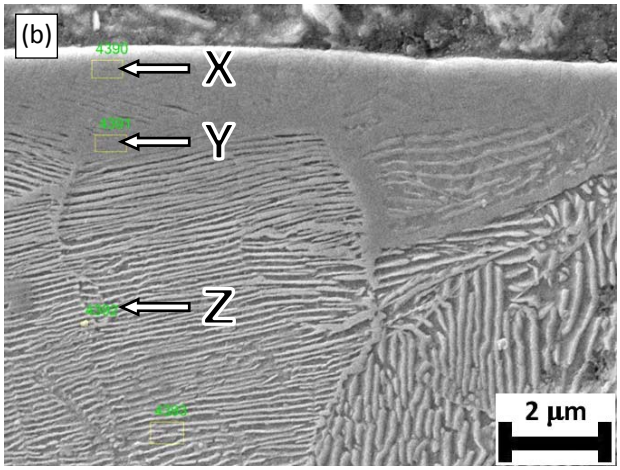

Element	Fe	C	N	Mn
X, at. %	81.28	14.13	3.40	1.14
Y, at. %	80.18	18.33	0.28	1.20
Z, at. %	79.59	19.27	–	1.14

Figure 6. SEM images of the steel treated at a temperature of 450 °C with: (a) 20 vol. % N_2 and (b) 80 vol. % N_2

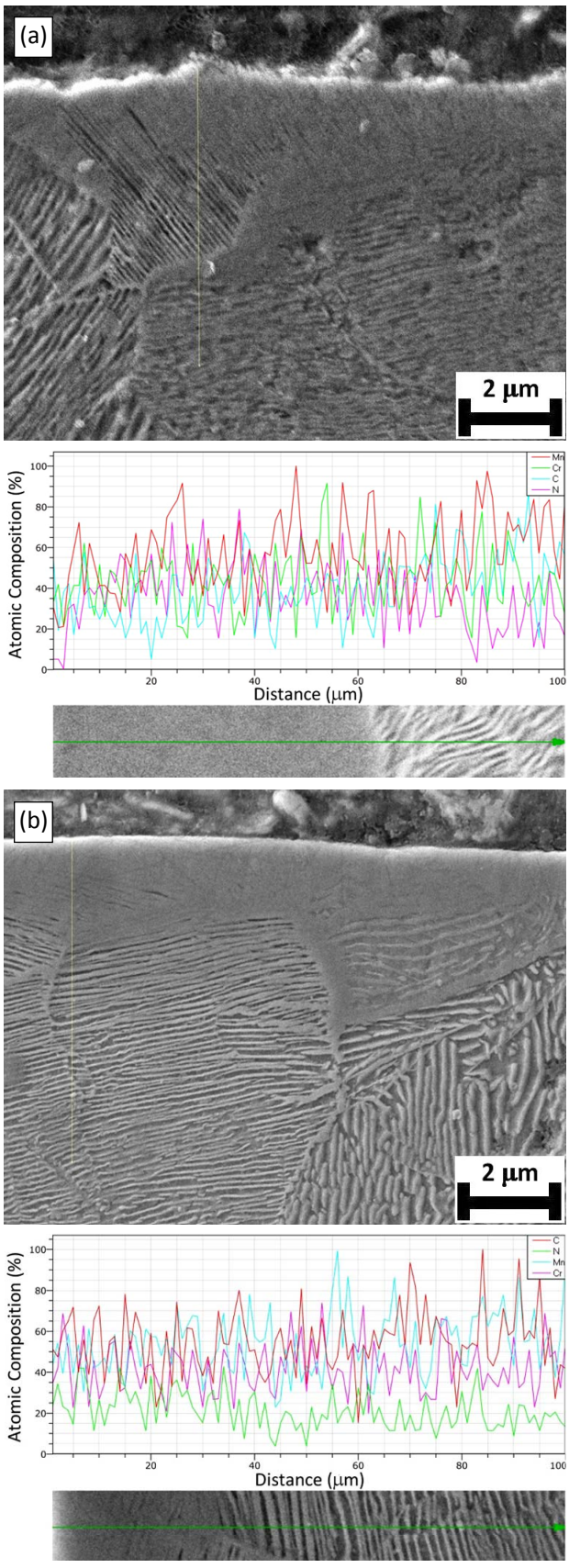

Figure 7. Elemental profiles in the diffusion zone of the steel treated at a temperature of 450 °C with: (a) 20 vol. % N_2 and (b) 80 vol. % N_2

R260 steel much rougher and helps nitrogen elements stick to it. This makes more nitrogen

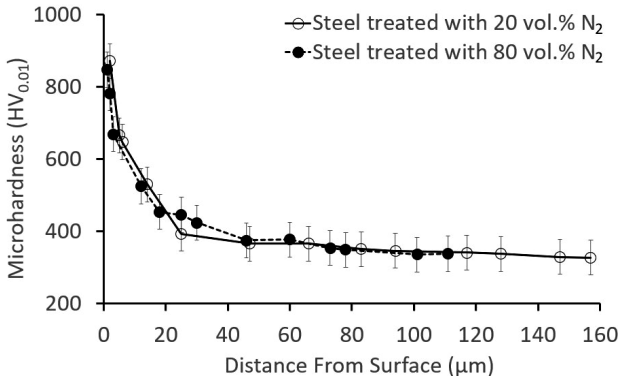

Figure 8. Cross-sectional hardness profiles of the steel treated at a temperature of 450 °C with 20 and 80 vol. % N_2

atoms in the ε-$Fe_{2-3}N$ and/or γ'-Fe_4N phases and changes the shape of the lattice [9]. The Volmer-Weber growth mode, which suggests that ion groups preferentially nucleate at defects caused by the nitriding process, could explain the increased surface roughness following treatment with higher nitrogen content in the gas composition with 80 vol. % N_2 [17]. The steel treated at 450 °C with 20 vol. % N_2 had a smoother appearance.

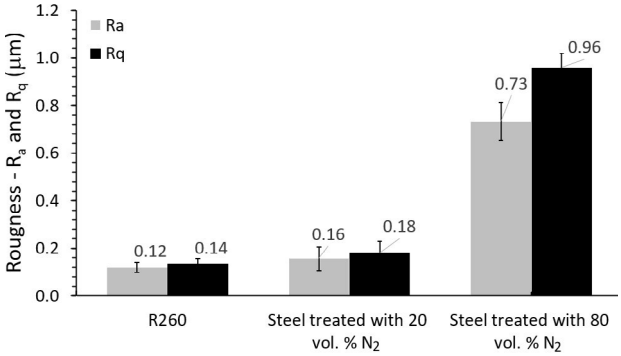

Figure 9. Roughness measurements in the untreated R260 and steel treated at a temperature of 450 °C with 20 and 80 vol. % N_2

Figure 10 shows the comparison of the wear volumes of the untreated R260 and steel treated at a temperature of 450 °C with 20 and 80 vol. % N_2 after the sliding distance of 57.5 m. A reciprocal tribological test showed that the HVOF sprayed AISI 316L stainless steel coating, nitrided at 450 °C, shows the best wear resistance under a 30 N load [18]. No significant difference was observed in the average wear volume between the three steel samples tested up to 30 N normal load. Generally, the wear volume increases as the load increases. More importantly, the wear at the steel treated at 450 °C with 80 vol. % N_2 maintains a lower wear volume.

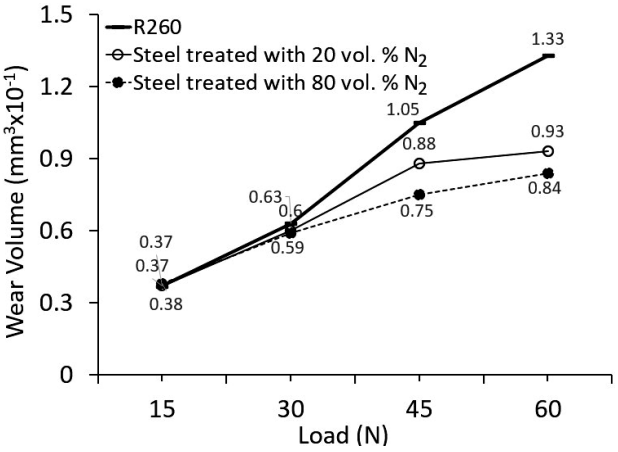

Figure 10. Comparison of the wear volumes of the untreated R260 and steel treated at a temperature of 450 °C with 20 and 80 vol. % N_2

Figure 11 shows the steel sample's coefficients of friction as a function of sliding distance and the steady-state CoF values after a 30 m sliding distance. Steel samples demonstrated a consistent variation in their coefficient of friction. No significant difference was observed in the average CoF of steel treated with 80 vol. % N_2 tested in the load range of 30 – 60 N. The CoF of steel treated with 20 vol. % N_2 tested in the load range of 15 – 60 N decreased with an increase in load (from 1.14 to 0.74). Contact under sliding conditions that generate wear is known to transform part of the friction-dissipated energy into heat, quickly promoting a significant increase in the temperature of the surfaces [19]. As the characterisation of worn surfaces will demonstrate, the reduction of the steady-state CoF with an increase in normal load can be associated with the formation of oxides on the surfaces. The present study results (CoF of about 0.8) with a normal load of 60 N and a sliding speed of 1.9 cm/s are similar to those found by Alemani et al. [20], even though the normal force, speed and counter-body were different.

LOM images of worn surfaces of the steel samples and corresponding Al_2O_3 balls (counter-body) for the two higher normal loads (45 N and 60 N) are shown in Figures 12 and 13. These figures clearly display two typical morphologies of worn surfaces. The main mechanisms found were adhesion and oxidation, with the latter increasing with the normal load. The wear for the steel treated with 80 vol. % N_2 is less severe than that for the other steel samples. The untreated R260 steel worn surface showed obvious peeling and spalling damage. Additionally, the damage was more intense in the untreated R260 steel than in

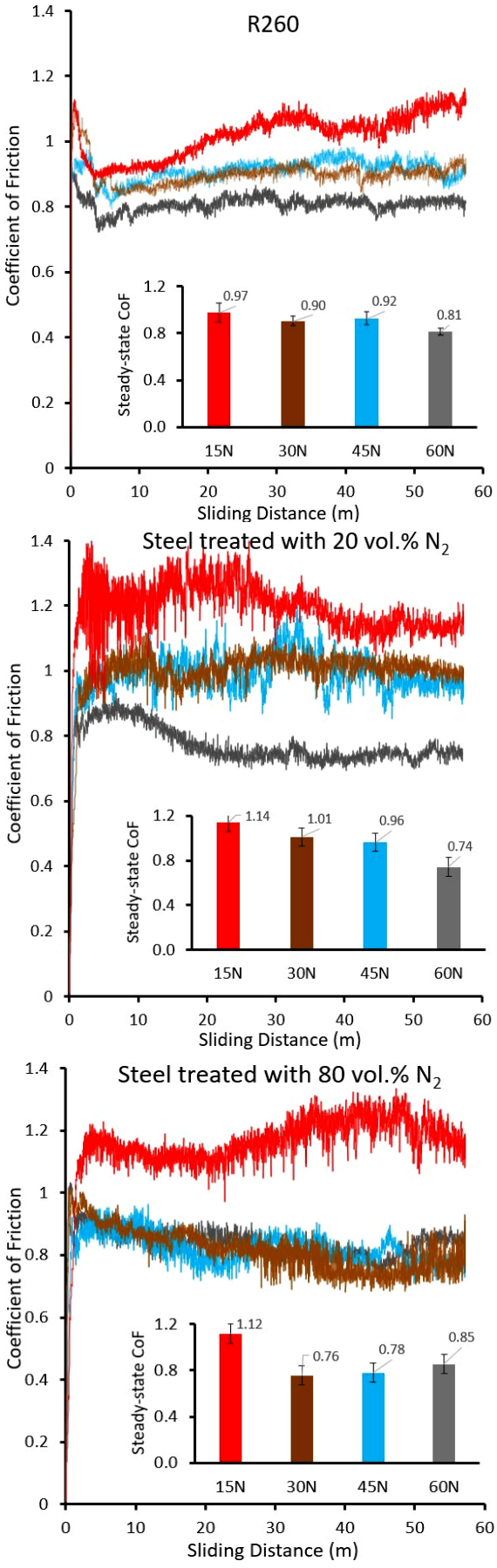

Figure 11. Coefficient of friction of the untreated R260 and steel treated with 20 and 80 vol. % N_2 as a function of sliding distance

the other nitrided steel samples, likely due to the low surface hardness (approximately 330 HV0.01) [1]. The oxidative mechanisms were more intense under the higher normal load condition. The increase in the normal load promotes an increase in the surface temperature, which results in a significant increase in the reactivity of the surfaces with the atmosphere. The grey areas indicate the presence of oxides and confirm the oxidative mechanism. Figure 13 shows a larger area with oxides on the worn surface after the test with a normal load of 60 N than with a normal load of 45 N. Due to the contrast difference, it was possible to quantify the area fraction with oxides. The increase in normal load from 45 to 60 N promoted an increase in the area fraction, with oxides changing from approx. 20 ± 5 % to approx. 40 ± 5 % for the steel treated with 20 vol. % N_2 and from approx. 40 ± 5 % to approx. 60 ± 5 % for the steel treated with 80 vol. % N_2. This result confirms the behaviour presented in Figure 11, where the CoF and fluctuation in the CoF decrease with the normal load.

It is important to mention that when comparing nitrided steel samples with different ratios of N_2 and H_2, the steel treated with 80 vol. % N_2 performed better than the steel treated with 20 vol. % N_2. The plasma nitriding process may have generated a larger compressive residual stress on the steel surface. Also, nitriding of the R260 rail steel caused elastic distortion (approx. 0.18 % for steel treated with 20 vol. % N_2 and approx. 2.14 % for steel treated with 80 vol. % N_2), which led to the formation of compressive residual stress as described by Leskovšek et al. [21]. The dissolved nitrogen in the pearlitic matrix correlated with lattice distortion for the R260 rail steel treated at 450 °C with 20 and 80 vol. % N_2 [22]. It is thought that when the steel treated with 20 vol. % N_2 was nitrided, the diffused nitrogen caused a large increase in the amount of incoherent nitrides in the diffusion zone. This decreased elastic lattice strain and compressive residual stress compared to steel treated with 80 vol. % N_2. Steel treated with 80 vol. % N_2 exhibited the best wear performance due to a thicker compound layer, a deeper hardened case and higher compressive residual stress within the nitride layer. In contrast, steel treated with 20 vol. % N_2 showed a shallower case-hardening depth, a thinner compound layer and a lower compressive residual stress. According to recent research by Valdés et al. [23], microstrain and compressive residual stress on the surface delay surface cracking and craters, improving wear resistance.

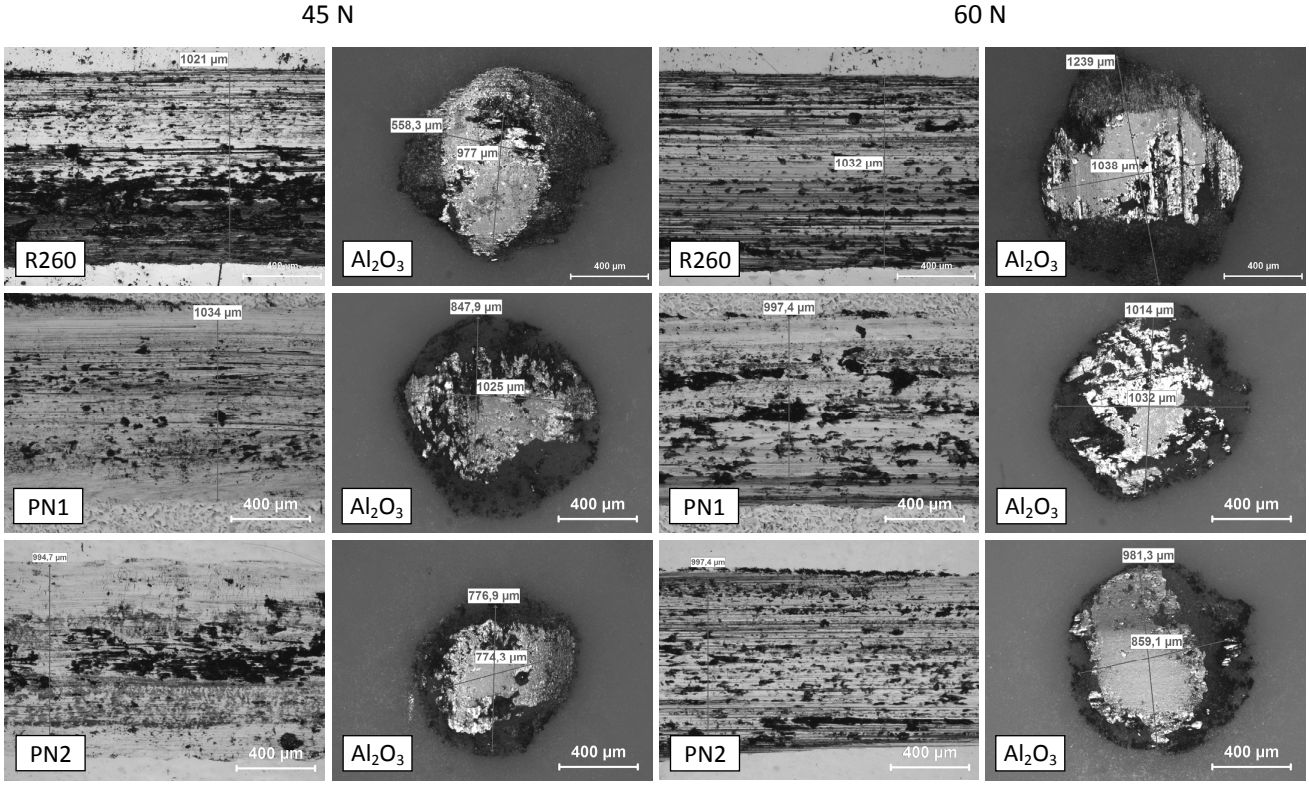

Figure 12. Lower magnification LOM images of the wear tracks generated at different normal loads on the surfaces of steel samples and corresponding counter-body Al_2O_3 balls after the tribological testing

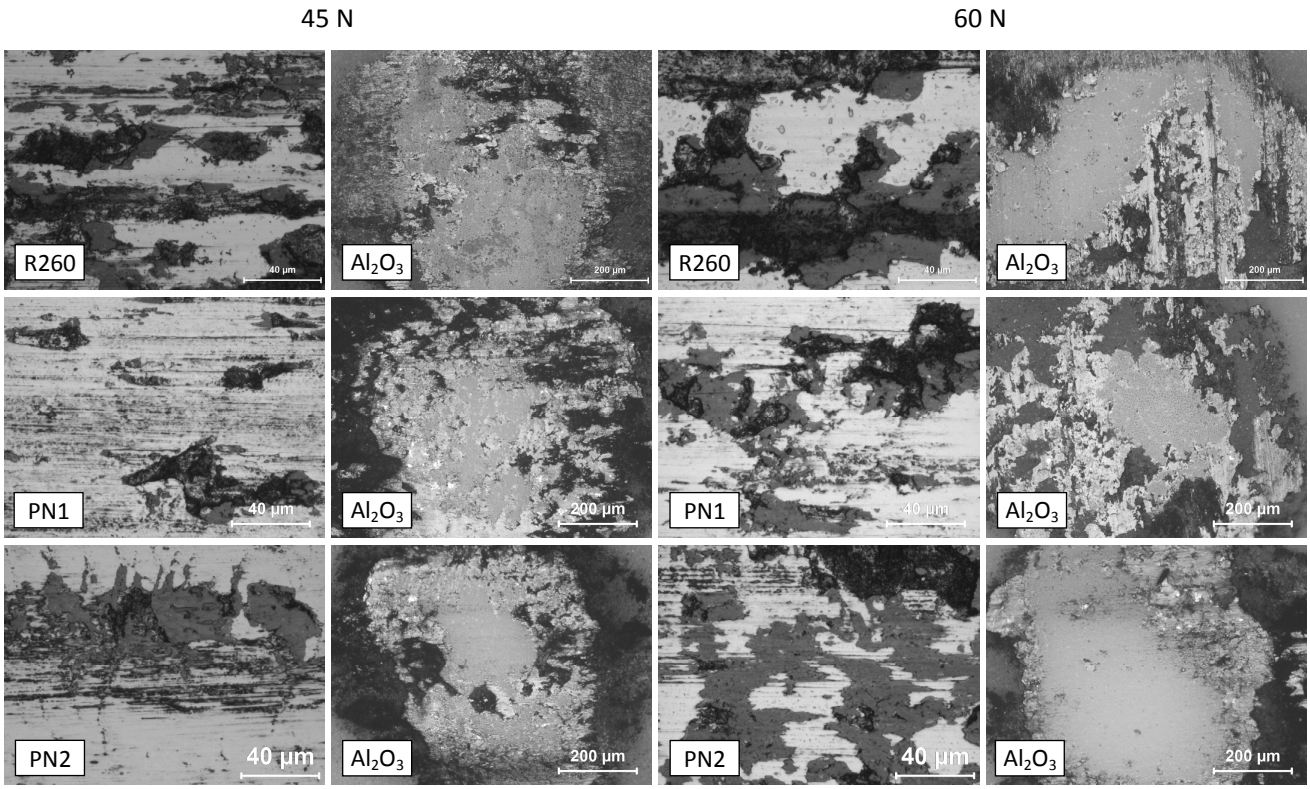

Figure 13. Higher magnification LOM images of the wear tracks generated at different normal loads on the surfaces of steel samples and corresponding counter-body Al_2O_3 balls after the tribological testing

4. Conclusion

This research assessed the effect of plasma nitriding on the tribological behaviour of R260 rail steel. The main conclusions could be drawn as follows:

- Plasma nitriding at 450 °C with N_2:H_2 volume ratios of 20:80 and 80:20 was successfully applied to the R260 rail steel. Cross-sectional LOM observations revealed compound layer thickness of approximately 2.58 and 5.37 µm for steel treated at 450 °C with 20 and 80 vol. % N_2, respectively. As the N_2 amount increased, the total compound layer thicknesses increased. There were no visible cracks.
- The steel treated at 450 °C with 20 and 80 vol. % N_2 exhibited a biphasic compound layer of ε-$Fe_{2-3}N$ and γ'-Fe_4N.
- The treatment with a nitrogen-rich gas composition (80 vol. % N_2) introduced more compressive residual stresses on the steel surface and roughened the surface compared to the composition containing 20 vol. % N_2.
- After plasma nitriding, the formation of iron nitrides such as ε-$Fe_{2-3}N$ and γ'-Fe_4N significantly improved the microhardness on the nitrided surface.
- In sliding applications, the steel treated with 80 vol. % N_2 showed better wear performance in the load range of 30 – 60 N when compared to steel treated with 20 vol. % N_2.

Future work will aim to compare the impact and sliding tribological performances of monophasic compound layer (γ'-Fe_4N) and biphasic compound layer (ε-$Fe_{2-3}N$ and γ'-Fe_4N) with thin and thick diffusion zone in the gas composition with the low and high nitrogen concentrations under extremely high contact pressures at room temperature.

Acknowledgement

This study was supported by the research foundation of Bilecik Şeyh Edebali University (Project No. 2023-01.BŞEÜ.03-02). We also extend our gratitude to Dr. Ersin E. Korkmaz for applying the plasma nitriding treatment to the steel.

References

[1] D.E.P. Klenam, L.H. Chown, M.J. Papo, L.A. Cornish, Steels for rail axles – An overview, Critical Reviews in Solid State and Materials Sciences, Vol. 49, No. 2, 2024, pp. 163-193, DOI: 10.1080/10408436.2022.2137462

[2] W. Bai, X. Xu, Y. Liu, Y. Liang, Y. Shen, Z. Han, Z. Sheng, R. Chen, M. Zhu, Microstructural

evolutions and impact toughness in simulated welding heat affected zones for a high-strength carbide-free bainitic rail steel, Materials Science and Engineering A, Vol. 880, 2023, Paper 145325, DOI: 10.1016/j.msea.2023.145325

[3] R. Stock, R. Pippan, RCF and wear in theory and practice – The influence of rail grade on wear and RCF, Wear, Vol. 271, No. 1-2, 2011, pp. 125-133, DOI: 10.1016/j.wear.2010.10.015

[4] Q. Wu, T. Qin, M. Shen, K. Rong, G. Xiong, J. Peng, Effect of gas nitriding on interface adhesion and surface damage of CL60 railway wheels under rolling contact conditions, Metals, Vol. 10, No. 7, 2020, Paper 911, DOI: 10.3390/met10070911

[5] Z. Orouji, S. Pour-Ali, R. Tavangar, Exploring microstructural evolution, nitrogen depth profile, and dry wear performance in 31CrMoV9 steel through combined severe shot peening and plasma nitriding, Materials Today Communications, Vol. 39, 2024, Paper 109182, DOI: 10.1016/j.mtcomm.2024.109182

[6] A.R. Mashreghi, S.M.Y. Soleimani, S. Saberifar, The investigation of wear and corrosion behavior of plasma nitrided DIN 1.2210 cold work tool steel, Materials & Design, Vol. 46, 2013, pp. 532-538, DOI: 10.1016/j.matdes.2012.10.046

[7] P. Landgraf, T. Bergelt, L.-M. Rymer, C. Kipp, T. Grund, G. Bräuer, T. Lampke, Evolution of microstructure and hardness of the nitrided zone during plasma nitriding of high-alloy tool steel, Metals, Vol. 12, No. 5, 2022, Paper 866, DOI: 10.3390/met12050866

[8] R.L. Dalcin, A. da Silva Rocha, V.V. de Castro, L.F. Oliveira, J.C.K. das Neves, C.H. da Silva, C. de Fraga Malfatti, Influence of plasma nitriding with a nitrogen rich gas composition on the reciprocating sliding wear of a DIN 18MnCrSiMo6-4 steel, Materials Research, Vol. 24, No. 4, 2021, Paper 20200592, DOI: 10.1590/1980-5373-MR-2020-0592

[9] R.L. Dalcin, A. da Silva Rocha, V.V. de Castro, J.C.K. das Neves, C.H. da Silva, R.D. Torres, R.M. Nunes, C. de Fraga Malfatti, Microstructure and wear properties of a low carbon bainitic steel on plasma nitriding at different N_2-H_2 gas mixtures, Materials Research, Vol. 25, 2022, Paper 20210447, DOI: 10.1590/1980-5373-MR-2021-0447

[10] R.L. Dalcin, V.M. de Menezes, L.F. Oliveira, C.H. da Silva, J.C.K. das Neves, C.A. Theis Soares Diehl, A. da Silva Rocha, Improvement on pitting wear resistance of gears by controlled forging and plasma nitriding, Journal of Materials Research and Technology, Vol. 18, 2022, pp. 4698-4713, DOI: 10.1016/j.jmrt.2022.04.122

[11] J. Sun, J. Li, J.M. Xie, Y. Yang, W.P. Wu, X. Zhou, S.H. Zhang, Q.M. Wang, Properties of rapid arc discharge plasma nitriding of AISI 420 martensitic stainless: Effect of nitriding temperatures, Journal of Materials Research and Technology, Vol. 19, 2022, pp. 4804-4814, DOI: 10.1016/j.jmrt.2022.07.028

[12] ASTM E92-17, Standard Test Methods for Vickers Hardness and Knoop Hardness of Metallic Materials, 2017.

[13] ISO 4287, Geometrical Product Specifications (GPS) – Surface Texture: Profile Method – Terms, Definitions and Surface Texture Parameters, 1997.

[14] ASTM G133-05, Standard Test Method for Linearly Reciprocating Ball-on-Flat Sliding Wear, 2005.

[15] S. Taktak, I. Gunes, S. Ulker, Y. Yalcin, Effect of N_2 + H_2 gas mixtures in plasma nitriding on tribological properties of duplex surface treated steels, Materials Characterization, Vol. 59, No. 12, 2008, pp. 1784-1791, DOI: 10.1016/j.matchar.2008.04.010

[16] ISO 2639, Steels – Determination and Verification of the Depth of Carburized and Hardened Cases, 2002.

[17] Y. Deng, C. Tan, Y. Wang, L. Chen, P. Cai, T. Kuang, S. Lei, K. Zhou, Effects of tailored nitriding layers on comprehensive properties of duplex plasma-treated AlTiN coatings, Ceramics International, Vol. 43, No. 12, 2017, pp. 8721-8729, DOI: 10.1016/j.ceramint.2017.03.209

[18] Z. Taskan, E. Ozturk, S. Tezcan, H. Mindivan, Influence of plasma nitriding on tribological performance of HVOF sprayed AISI 316L and AISI 420 stainless steel coatings, Tribology and Materials, Vol. 3, No. 4, 2024, pp. 187-196, DOI: 10.46793/tribomat.2024.020

[19] Y.-x. Peng, X.-d. Chang, S.-s. Sun, Z.-c. Zhu, X.-s. Gong, S.-y. Zou, W.-x. Xu, Z.-T. Mi, The friction and wear properties of steel wire rope sliding against itself under impact load, Wear, Vol. 400-401, 2018, pp. 194-206, DOI: 10.1016/j.wear.2018.01.010

[20] M. Alemani, S. Gialanella, G. Straffelini, R. Ciudin, U. Olofsson, G. Perricone, I. Metinoz, Dry sliding of a low steel friction material against cast iron at different loads: Characterization of the friction layer and wear debris, Wear, Vol. 376-377, No. B, 2017, pp. 1450-1459, DOI: 10.1016/j.wear.2017.01.040

[21] V. Leskovšek, B. Podgornik, D. Nolan, Modelling of residual stress profiles in plasma nitrided tool steel, Materials Characterization, Vol. 59, No. 4, 2008, pp. 454-461, DOI: 10.1016/j.matchar.2007.03.009

[22] K.T. Cho, K. Song, S.H. Oh, Y.-K. Lee, W.B. Lee, Surface hardening of shot peened H13 steel by enhanced nitrogen diffusion, Surface and

Coatings Technology, Vol. 232, 2013, pp. 912-919, DOI: 10.1016/j.surfcoat.2013.06.123

[23] J. Valdés, J. Solis, R. Mercado, J. Oseguera, H. Carreón, C. Aguilar, A. Medina, Influence of plasma nitriding treatment on the micro-scale abrasive wear behavior of AISI 4140 steel, Materials Letters, Vol. 324, 2022, Paper 132629, DOI: 10.1016/j.matlet.2022.132629